Temporal patterns of fire density by vegetation type and region in Mexico and its temporal relationships with a monthly satellite fuel greenness index

Vega-Nieva D.J.[1], Nava-Miranda M.G.[1*], Calleros-Flores E.[1], López-Serrano P.M.[1], Briseño-Reyes J.[1], López-Sánchez C.[1], Corral-Rivas, J.J.[1], Montiel-Antuna E.[1], Alvarado-Celestino E.[2], González-Cabán A.[3], Cruz I.,[4] Ressl, R.[4], Cortes-Montaño C.[1], Pérez-Salicrup D.[5], Jardel-Pelaez E.[6], Jiménez E.[7], Arellano-Pérez S.[8], Álvarez-González J.G.[8], Ruiz-González A.D.[8]

[1] Facultad de Ciencias Forestales. Universidad Juárez del Estado de Durango (México),

[2] School of Environmental and Forest Sciences. University of Washington,

[3] Pacific Southwest Research Station. US Department of Agriculture Forest Service,

[4] Comisión Nacional para el Conocimiento y Uso de la Biodiversidad (CONABIO),

[5] Universidad Autónoma de México (México),

[6] Universidad de Guadalajara (México),

[7] Centro de Investigación Forestal – Lourizán, Xunta de Galicia (Spain),

[8] Unidad de Gestión Forestal Sostenible. Departamento de Ingeniería Agroforestal. Universidad de Santiago de Compostela. Lugo, Spain

*corresponding author. Email: nava.miranda@gmail.com

ABSTRACT

Understanding the temporal patterns of fire occurrence and their relationships with fuel dryness is key for a sound fire management, especially under increasing global warming. At present, no system for prediction of fire occurrence risk is available in Mexico based on fuel dryness conditions. As part of an ongoing national scale project, we developed an operational fire risk and danger mapping tool based on satellite and weather information. We demonstrate how differing monthly temporal trends in a fuel greenness index, dead ratio (DR) and fire density (FDI) can be clearly differentiated by vegetation type and region for the whole country, using MODIS satellite observations for the period 2003-2014. We tested linear and non-linear models, including temporal autocorrelation terms, for prediction of FDI from DR for a total of 28 combinations of vegetation types and regions. In addition, we developed seasonal autoregressive integrated moving average (ARIMA) models for forecasting of DR values based on the last observed values. Most ARIMA models showed values of the adjusted coefficient of determination (R^2 adj) above 0.7-0.8, suggesting potential to forecast fuel dryness and fire risk and danger conditions. The best fitted models explained more than 70% of the observed FDI variation in the relation between monthly DR and fire density. These results suggest the potential of this index to be incorporated in future fire risk operational tools. However, some vegetation types and regions show lower correlations between DR and observed fire density, suggesting that other variables, such as distance and timing of agricultural burn, deserve attention in future studies.

RESUMEN

Una adecuada planificación del manejo del fuego requiere de la comprensión de los patrones temporales de humedad del combustible y su influencia en el riesgo de incendio, particularmente bajo un escenario de calentamiento global. En la actualidad en México no existe ningún sistema operacional para la predicción del riesgo de incendio en base al grado de estrés hídrico de los combustibles. Un proyecto de investigación nacional actualmente en funcionamiento, tiene como objetivo el desarrollo de un sistema operacional de riesgo y peligro de incendio en base a información meteorológica y de satélite para México. Este estudio pertenece al citado proyecto, y muestra cómo se pueden distinguir en el país distintas tendencias temporales en un índice de estrés hídrico de los combustibles basado en imágenes MODIS, el índice DR, y en las tendencias temporales de densidad de incendios, en distintos tipos de vegetación y regiones del país. Se evaluaron varios modelos lineales y potenciales, incluyendo términos para la consideración de la autocorrelación temporal, para la predicción de la densidad de incendios a partir del índice DR para un total de 28 tipos de vegetación y regiones. Se desarrollaron además modelos estacionales autorregresivos de media móvil (ARIMA) para el pronóstico del índice DR a partir de los últimos valores observados. La mayoría de los modelos ARIMA desarrollados mostraron valores del coeficiente de determinación ajustado (R^2 adj.) por encima de 0.7-0.8, sugiriendo potencial para ser empleados para un pronóstico del estrés hídrico de los combustibles y las condiciones de riesgo y peligro de incendio. Con respecto a los modelos que relacionan los valores mensuales de DR con FDI, la mayoría de ellos explicaron más del 70% de la variabilidad observada en FDI, sugiriendo potencial de este índice para ser incluido en futuras herramientas operacionales de riesgo de incendio. En algunos tipos de vegetación y regiones se obtuvieron correlaciones más reducidas entre el índice DR y los valores observados de densidad de incendios, sugiriendo que el papel de otras variables tales como la distancia y el patrón temporal de quemas agrícolas debería ser explorado en futuros estudios.

INTRODUCTION

Understanding of temporal patterns of fire occurrence and their relationships with fuel dryness is key for sound fire management, especially under increased global warming, which may result in increasing drought conditions and potentially increasing fire severity and frequency in some regions (e.g. Wotton *et al*. 2003; Gillet *et al*. 2004; Flanningan *et al*. 2006, 2009; Woolford *et al*. 2013).

Satellite sensors have been utilized in the last years to monitor fuel greenness and associated fire risk and danger (Lozano *et al*. 2007, 2008; Chuvieco *et al*. 2004, 2010; López *et al*. 2012; Yebra *et al*. 2008, 2013). Some systems such as the Fire Potential Index (FPI) (Burgan *et al*. 1998) have integrated satellite information by means of fuel greenness indices based on relative values of the Normalized Difference Vegetation Index (NDVI) for each vegetation type (Burgan and Hartford 1993; Burgan *et al*. 1996, 1997, 1998), combined with daily 10 h fuel moisture content calculated from observations of weather stations (Fosberg and Deeming 1971) to map fuel greenness and associated fire risk and danger. Such fire danger systems offer useful information for a sound decision-making in strategic fire management planning (e.g. Preisler *et al*. 2011, Mavsar *et al*. 2013, Rodríguez y Silva *et al*. 2014). These operational fire danger systems have largely been utilized in the United States of America (USA) (Burgan *et al*. 1998; Preisler and Westerling 2007; Preisler *et al*. 2009, 2015) or in the European continent (Sebastian-Lopez *et al*. 2002) including Spain (Huesca *et al*. 2007, 2009, 2014).

In Mexico, Sepúlveda *et al*. (1999, 2001) tested the FPI system (Burgan *et al*. 1998) in the Baja California region, and Manzo-Delgado *et al*. (2004, 2009) demonstrated the potential of the temporal evolution of NDVI-based indices as indicators of fuel drought and associated fire risk in central Mexico.

In addition to these pioneering studies, previous work on fire risk in Mexico has focused on the influence of climate and fuels at regional and local scales. Several studies analyzed climatic effects on fire regimes (e.g. Heyerdahl and Alvarado 2003; Fulè *et al*. 2005, Drury and Veblen 2008, Skinner *et al*. 2008, Návar-Cháidez and Lizárraga-Mendiola 2013). Others evaluated the role of weather variables such as precipitation or temperature (e.g. Carrillo García *et al*. 2012; Avila-Flores et al. 2010a, 2010b; Antonio and Ellis 2015), or weather-based fire danger indices (e.g. Villers et al., 2012) on fire occurrence risk, mainly at local or regional scales. Some local or regional studies also considered the influence of fuels on fire occurrence risk (e.g. Flores Garnica *et al*. 1990, Muñoz Robles *et al*. 2005, Wong González and Villers Ruiz 2007, Castañeda Rojas *et al*. 2015). Whereas previous research offers useful information specific to the scale of their regions of study, there is a need for studies analyzing fire risk and its relationships with fuel dryness spatial and temporal patterns at a national scale, that cover the ample diversity of climatic and environmental conditions of Mexico (González- Cabán and Sandberg 1989, Cerano Paredes *et al*. 2010). Specifically, no operational fire danger system is currently available in Mexico. This in contrast with countries such as USA, Canada or Brazil that have developed operational fire risk systems based on temporal and spatial quantification of fuel greenness and associated fire risk and danger (e.g. Deeming *et al*. 1977; Van Wagner 1987; Burgan *et al*. 1997, 1998; Preisler *et al*. 2004, 2008, 2011; 2013; Setzer and Sismanoglu 2012; Riley *et al*. 2013). This lack of an operational fire danger system led the Forest National Commission (CONAFOR in Spanish) and the National Research Agency (CONACYT in Spanish) to fund the national scale project "Development of a Fire Danger System for Mexico". The main objective of the study is the development of an operational fire risk and danger mapping system based on satellite and weather information for Mexico (Vega-Nieva *et al*. 2015).

Within the frame of the research project, the present study focuses on understanding temporal patterns of fire density by vegetation type and region in Mexico and exploring its relationships with a MODIS-based fuel greenness index. The specific objectives of the study are:

1) To quantify the monthly temporal trends of a MODIS satellite based fuel greenness index, DR, and the temporal trends of fire density (FD) by vegetation type and region in Mexico.

2) To test regression models, including temporal autocorrelation of residues, for prediction of monthly FD by vegetation type and region from monthly DR values in Mexico.

3) To develop autoregressive integrated moving average (ARIMA) models that can be utilized for forecasting DR based on the last observed values of this index.

METHODS

Study Area

Because of the national scope of the work, the area of study was the Mexican Republic. Figure 1 shows the vegetation types present in the country according to the National Institute of Geography and Statistics (INEGI in Spanish) most recent land use map **(**INEGI Land Use Map Series V, 1:25000 http://www.inegi.org.mx/geo/contenidos/recnat/usosuelo/).

We reclassified vegetation types into the following 7 categories: Agriculture (AG); Arboreous Secondary Vegetation (ARBSV); Deciduous Tropical Forest (DTROPF); Pastureland (PAS); Perennial Tropical Forest (PTROPF); Shrubby Secondary Vegetation (SHSV) and Temperate Forest (TFOR).

Given the well-documented variations in fire regimes seasonality in the country (e.g. Rodriguez-Trejo *et al*. 2008; Yocom *et al*. 2010, 2012, 2014; Jardel *et al*. 2014), four geographical regions, Northwest (NW), Northeast (NE), Center (C), and South (S), were established (figure 1). The regions definition was based on the potential fire regimes zoning for Mexico (Jardel *et al*. 2014), as well as vegetation types and climatic zones (Holridge 1996), together with a visual observation of the temporal and spatial patterns of clustering in fire hotspots for the period of study. The seven vegetation types defined above were present in all 4 regions, resulting in a total of 28 combinations of vegetation types and region to be modeled.

MODIS monthly fire hotspots and NDVI data

Considering the availability of MODIS fire hot spots information for Mexico we selected the period of 2003-2014 for our study. We compiled monthly MODIS fire hotspots for the 12 years of the study period from CONABIO (http://incendios1.conabio.gob.mx/). Data were filtered to avoid false detections from constant heat sources such as factories. The monthly NDVI composite images with a spatial resolution of 1 x 1 km (MODIS product MOD13A3) from the study period were downloaded from http://modis.gsfc.nasa.gov/data/dataprod/mod13.php.

Dead Ratio calculation

Following Burgan *et al*. (1998), the following Dead Ratio index was calculated:

$$DR = 100 - LR \quad (1)$$

Where: DR= Dead Ratio, LR= Live ratio

Dead ratio is an empirical index representing the fraction of fuel that is not alive, reaching 100 in a fuel that is completely cured with no live biomass, and with lower values representing fuels with a higher fraction of live biomass. Its calculation is based on relative greenness values and maximum live ratios following Burgan *et al*. (1998) equations 2 to 4:

$$LR = RG * LR_{max} /100 \quad (2)$$

Where: RG is Relative Greenness, and calculated as:

$$RG = (NDVI_0-NDVI_{min})/(NDVI_{max}-NDVI_{min})*100 \quad (3)$$

Where: $NDVI_0$ the observed NDVI for each pixel at every month, $NDVI_{min}$ and $NDVI_{max}$ are the minimum and maximum NDVI values for each pixel. LR_{max} is the maximum Live Ratio and calculated as:

$$LR_{max}=35+40*(NDVI_{max}-125)/(255-125) \quad (4)$$

The values 125 and 255 are the absolute minimum and maximum NDVI values observed for Mexico. Maximum and minimum NDVI values for each pixel and absolute minimum and maximum NDVI values were calculated considering all the NDVI monthly images for the period 2003-2014. Dead Ratio (DR) values were calculated for each monthly NDVI image in the period of study and mean DR value for each monthly image was calculated using Cell Statistics in ArcGIS 10.3 (ESRI 2011).

Fire Density Index

For each of the 28 vegetation types and regions considered, monthly Fire Density (FD) was calculated by dividing the number of fires in the area by the surface (km^2) of the vegetation/region considered. Monthly FD values for each vegetation type and region were scaled to a Fire Density Index (FDI) as follows:

$$FDI= \text{Number of fires} / \text{Surface } (km^2) \times 5000 \quad (5)$$

The FDI index is defined so that a FD of 0.01 fires/km^2 – e.g. 1 fire/100 km^2 – is equivalent to an FDI value of 50. Accordingly, a FD of 2 fires/100 km^2 is equivalent to an FDI value of 100, which might be considered an indicator of a high fire density.

Modeling monthly FDI from DR

Except for agriculture, fire season concentrated on the period December-June for all vegetation types considered. Agriculture showed an earlier start of fire season, caused by agricultural burnings which usually take place very early on the dry season (Martínez-Torres et al. 2016). Consequently, all land uses, except for agriculture, were modeled for the period December-June and agriculture was modeled for the whole year.

Model formulation and selection.

We fitted linear and non-linear (power) models for prediction of FDI from DR for each vegetation type and region, following:

$$FDI = a_i + b_i * DR \tag{6}$$

$$FDI = a_0 * DR^{b0} \tag{7}$$

Where:

a_i, b_i, a_0, b_0, are model coefficients, *FDI:* Fire Density Index (eq. 5), *DR:* Dry Ratio (eq. 1).

To further assess whether the models are different among different months or groups of months, the nonlinear extra sum of squares method was used (Bates and Watts, 1988, pp. 103-104). This method requires the fitting of full and reduced models and has frequently been applied to assess whether separate models are necessary for different species or different geographic regions (e.g., Huang et al., 2000; Zhang et al., 2002; Corral et al., 2004; Castedo et al., 2005; Corral et al., 2007). In this paper the reduced model corresponds to the same set of global parameters for all months, as shown in eqs 6 and 7. The full models correspond to different sets of global parameters for different months or group of months which are obtained by expanding each global parameter by including an associated parameter and a dummy variable to differentiate the months or groups of months.

For example, the expansion of a global parameter b_i of a linear model (eq.6 for the reduced model) can be written as:

$$b_{i1}+b_{i2}d_2+\ldots+b_{i12}d_{12} \quad (8)$$

where $b_{i1}-b_{i5}$ are the associated parameters of the full model, and d_2–d_{12} are the dummy categorical variables for considering the months, which are defined as follows: $d_2 = 1$ if month = *February*, otherwise $d_2 = 0$; …; $d_2 = 12$ if month = *December*, otherwise $d_{12} = 0$;

The appropriate test statistic uses the following expression:

$$F = \frac{SSE_R - SSE_F}{df_R - df_F} \div \frac{SSE_F}{df_F} \quad (9)$$

where SSE_R is the error sum of squares of the reduced model, SSE_F is the error sum of squares of the full model, and df_R and df_F are the degrees of freedom of the full and reduced models, respectively. The non-linear extra sum of squares follows an *F*-distribution.

If the above F-test results reveal that there is no difference among the models for different months, a composite model fitted on the combined data is all that is needed. If the *F*-test results show that there are differences among models (P<0.05) further tests are needed to evaluate whether the differences are caused by as few as two or as many as all of the months. For instance, full models for all combinations of grouped months (1 to 11 grouped months for agriculture and 1 to 6 grouped months for the remaining vegetation types) were compared with their corresponding reduced model using the F-test. Only when an insignificant *F*-value (P>0.05) was obtained, the models for these two group of months could be considered similar and combined.

We selected candidate models where the grouped coefficients were significantly different as detected by the *F*-test. These candidate models were further evaluated by the following goodness of fit statistic statistics: adjusted coefficient of determination (R^2), root mean squared error (RMSE) and the Standard AIC, calculated as follows:

$$R^2_{adj} = 1 - \frac{(n-1)\sum(y_i - \hat{y}_i)^2}{(n-p)\sum(y_i - \bar{y})^2} \quad (10)$$

$$RMSE = \sqrt{\frac{\sum(y_i - \hat{y}_i)^2}{n-p}} \quad (11)$$

$$AIC = n \cdot \ln \hat{\sigma}^2 + 2 \cdot l - n \cdot \ln \hat{\sigma}^2 + 2 \cdot l \quad (12)$$

Where: y_i and $\hat{y}_i$ are the observed and estimated values of the dependent variable, respectively, $\bar{y}$ is the average value of the dependent variable, n is the total number of observations used to fit the model, p is the number of model parameters, l = p+1, and $\hat{\sigma}^2$ is the estimator of the error variance of the model the value of which is obtained as follows:

$$\hat{\sigma}^2 = \sum_{i=1}^{n} (y_i - \hat{y}_i)^2 / n \quad (13)$$

Autocorrelation

Because the structure of the data includes consecutive observations of FDI, autocorrelation within the residuals of each vegetation type/region might be expected, which would violate the assumption of independent error terms. In order to account for this temporal autocorrelation the adjustment was performed in two stages. First we adjusted models without accounting for the correlation between consecutive observations. We then examined presence of autocorrelation based on the visual inspection of plots of residuals against residuals from previous observations for each combination of vegetation type and region. Based on the observed autocorrelation at time lags of order k, we included a modified k-order autoregressive error structure which accounted for the time lag between consecutive observations in the models for each combination of vegetation type and region. Error terms were consequently expanded as follows:

$$e_i = \sum_{k=1}^{x} I_k \rho_k^{h_i - h_{i-k}} e_{i-k} + \varepsilon_i \tag{14}$$

where $I_k = 1$ for $i > k$ and it is zero for $i = k$, ρ_k is the k-order continuous autoregressive parameter to be estimated, and h_i-h_{i-k} is the time lag length (months) separating the ith from the ith-k observations, $h_i > h_{i-k}$, e_i is the ith ordinary residual (i.e., the difference between the observed and the estimated FDI at month i) for each combination of vegetation type and region.

The order k of the modified error structure was selected based on the plots of residuals against lag residuals. Models were fitted by use of the Model Procedure of SAS/ETS® (SAS Institute Inc. 2009).

Autoregressive integrated moving average (ARIMA) modeling of DR

We tested the fitting of seasonal AutoRegressive (AR) Integrated (I) Moving Average (MA) models (ARIMA) for forecasting the DR time series of each vegetation type and region. Seasonal ARIMAS are commonly utilized in the remote sensing domain due to the highly significant seasonal component usually associated with remote sensing time series (e.g. Fernández-Manso *et al*. 2011, Huesca *et al*. 2014).

The seasonal ARIMA model incorporates both non-seasonal and seasonal factors in a multiplicative model. One shorthand notation for the model is:

ARIMA (*ar, dif, ma*) × (*sar, sdif, sma*)*S*, (15)

with *ar* = non-seasonal AR lag order; *dif* = non-seasonal differencing; *ma* = non-seasonal MA lag order; *sar* = seasonal AR lag order; *sdif* = seasonal differencing; *sma* = seasonal MA lag order and *S* = time span of repeating seasonal pattern.

Seasonal ARIMA models were fitted using the "auto.arima" command within the library "forecasting" in R (Hyndman 2016, R Core Team 2016). The Standard AIC selection criterium (Hamilton 1994) was applied to select the most suitable model. The individual and joint significance of the model parameters was assessed by means of the Student-t and F tests.

We examined autocorrelation by plotting regular and partial autocorrelation functions (ACF and PACF) for both the variable DR to be adjusted and the residuals obtained by the ARIMA models. PACF and ACF plots of both DR and model residuals were obtained using the library "forecasting" in R (Hyndman 2016, R Core Team 2016). We selected models of the lowest AIC where no autocorrelation in the residuals was present as observed in Partial Autocorrelation Function (PACF) and Autocorrelation Function (ACF) plots.

RESULTS

Observed temporal trends of monthly DR and FDI

Figure 2 (captures at high resolution included as annexes) shows the observed temporal trends of the monthly mean DR values (upper lines, right axis) together with monthly FDI values (lower line, left axis) observed for each one of the 28 combinations of vegetation types and regions for the period of 12 years that was considered in the study.

Observed DR temporal trends by vegetation types and regions

For vegetation types, the highest DR values were observed in agricultural and pasture, and the lower DR values were found for all tropical forests, whereas temperate forests showed intermediate DR values. For most vegetation types, a regional gradient was observed with the highest DR values found in the NW region and lowest values in the S, with C and NE regions showing intermediate values. During the first months of the year all vegetation types and regions showed increasing DR values. The patterns of DR increase in these earlier months varied largely between vegetation types and regions. In general, the increase of DR occurred earlier for NW region compared to Central (C) and S regions. The rates of DR decrease, likely caused by the occurrence of precipitation, also varied largely by vegetation type and region. The decrease of the DR occurred earliest at the center and south regions for most of the vegetation types, often peaking at the months of April-May, and decreasing in the following months. In the NW region, the decrease of DR tended to occur later than the other regions, with NE showing intermediate values.

Observed FDI trends by vegetation types and regions

FDI values varied largely between vegetation types and regions. The highest FDI values were observed for agriculture, pasture and shrubby secondary vegetation in the S region, with values >500 (equivalent to a fire density of >10 fire hotspots/100 km^2).

The central region also showed high FDI values for most of the vegetation types, with maximum FDI values > 250 (> 5 fire hotspots /100 km^2) for most land uses.

In the NW, the highest FDI values were found for temperate forest, with FDI values >300 (equivalent to >6 fires/ km^2) In the NE region, observed FDI on temperate forest was lower than in the NW, with observed FDI values < 50 (< 1 fire hotspot/100 km^2) for most of the years.

Arboreous and shrubby secondary vegetation showed high FDI values for all of the regions, with C and S region reaching values above 100 in all years, and with values above 50 for NW and NE regions.

Regarding tropical forests, high FDI values > 100 and even > 200 were found in the driest years for deciduous tropical forests (DTROPF) in the four regions. Observed FDI values were generally two or three times higher than corresponding values for perennial tropical forests (PTROPF) in the NW, NE and S regions (figure 2). In the central region, in spite of lower DR conditions in PTROPF compared to DTROPF as expected in a wetter ecosystem, observed FDI values were high at both ecosystem types.

Models relating monthly FDI with DR by vegetation type and region

Both linear and power reduced models –those with common parameters for all months- (i.e. equations 7 and 8) resulted in R^2 values lower than 0.5 for all land uses, with the exception of pasture (PAS) from the NO region and deciduous tropical forests DTROPF of the S region, that could be modeled with a reduced non-linear model with all months grouped (eq. 7, table 2). For the remaining vegetation types, the F statistic calculated with full models was 10.4, and the probability of finding a critical value greater than 10.4 (i.e., Fcritical (1-α; dfR-dfF)>10.4) was lower than 0.01. There were therefore differences among the models from different months or groups of months.

Based on the F-tests and the evaluation of their goodness of fit statistics, we selected the models shown in table 1 as the best candidate models for each vegetation type and region. Fitted model coefficients for the selected best models are shown in Table 2. Nonlinear (power) models described the data better than linear models for all vegetation types and regions. Eqs. 7 and 16-24, with grouped coefficients for the earlier months (December to February, Mach or April) best fitted the data for non-agricultural vegetation types. Most models show separated coefficients for the peak months April or May, varying by vegetation type and region. In the case of agriculture (which was modeled for the 12 months), months of September to March or April could be grouped, suggesting a constant relationships of DR to FDI at the start of the fire season, with latter months (May, June and in some regions also April) having higher fire occurrence as noted by higher coefficient values for those latter months (eq. 25-27, table 2).

Predicted and observed FDI values for each vegetation type and region are shown in **Figure 3**. Goodness of fit statistics for the best fit models are shown in table 2. The selected equations showed good fits for several vegetation types and regions, with 13 of 28 models showing adjusted R^2 values higher than 0.8; 11 models in the range 0.7-0.8, and 4 models (those for temperate and tropical forests of the NE region and pasture of the NO) with adjusted R^2 values ranging from 0.65 to 0.7.

Autocorrelation in FDI models

A visual examination of the residuals at time *i* against the corresponding residuals at precedent months *i-k,* showed that residuals were correlated at time lag *k*=1 (i.e. with the previous month). No correlation was observed for the residuals for time lags *k* greater than 1 month for any vegetation type. Table 2 shows the *rho* parameter included in the models to account for temporal autocorrelation of the residuals.

Autoregressive integrated moving average (ARIMA) modeling of DR.

The best fit ARIMA models and goodness of fit coefficients are shown in Table 3. The best fit seasonal ARIMA models showed good adjusted R^2 values, with 14 models with R^2 values higher than 0.8; 9 models with adjusted R^2 values of 0-7-0.8, and 5 models (SHSV_S, PAS_S, ARBSV_S, PAS_NE, PTROPF_NE and PTROPF_S) with adjusted R^2 values of 0.6-0.7. RMSE values ranged from < 15 for 13 models, <25 for a total of 24 models, with the remaining 4 models ranging between 25-35 (DTROPF_NE, AG_S, PAS_S, DTROPF_NW).

The order of the non-seasonal autoregressive coefficients (*ar*) ranged from 1 to 6 months, often corresponding to the correlation lags suggested by the Partial Autocorrelation Function

(PACF) and Autocorrelation Function (ACF) plots of DR. No integrated coefficients (*dif* and *sdif*) were obtained for any model, as expected due to the absence of differencing in the variable to be modeled. Some of the best fit models included moving average (*ma*) coefficients of order 1-2, and seasonal autorregresive (*sar*) and moving average (*sma*) coefficients of order 1-2 and 1-3, respectively. For all the models, we plotted ACF and PACF of the variable DR to be adjusted, and also of the residuals after adjustment, to inspect the presence of partial or absolute correlation at any time lag after adjustment. Figure 4 shows an example of ACF and PACF plots of DR and of the best fit ARMA model residual. ACF and PACF plots for all vegetation types are included as annexes. For all vegetation types, correlations at time lags ranging from 1 to 6 months were visible in the PACF and ACF plots of the DR variable to be modeled. This correlation was removed in the residuals of the best fit models, with PACF and ACF values below the level for significant correlation at all time lags (Fig 4 and annexes).

Mapping predicted fire occurrence risk

We produced maps of predicted FDI from DR based on the best fit models for each vegetation type. Figure 5 (captures at high resolution included as annexes) shows an example of predicted FDI maps for the fire season months of March to June for two contrasting years: 2010, a more moderate fire year, and 2011, an extremely dry year with a large fire occurrence. It can be seen that the different fuel drought conditions result in very contrasting FDI predictions between the two years. In the year 2011, predicted FDI was high to extreme for the months of April and May for the NW and NE regions, corresponding with a very high hotspot density observed on those two regions and contrasting with lower predicted FDI and observed hotspot density for the same months in the year 2010. Fire risk in the central region was also higher in 2011, with higher predicted and observed fire density in the months of March to May. In the South region, fuel drought and associated FDI were also higher in the year 2011, particularly in the months of May and June, corresponding with a higher observed hotspot density.

DISCUSSION

Observed DR temporal trends by vegetation types and regions

The DR trend with vegetation types suggest sensitivity of this index to the different moisture conditions at different ecosystem types, with the highest values observed for pasture and agriculture while the lowest DR values measured in more humid ecosystems such as perennial tropical forests. The relative greenness component of the index is designed to normalize the index value between land types. However, by multiplying relative greenness by a maximum live ratio which depends on the maximum NDVI (Burgan *et al*. 1998), the DR index takes into account the variability due to type of vegetation. Different types of vegetation have different seasonal trends of drying and wetting, which is reflected into their NDVI temporal trends (e.g. Yebra *et al*. 2008). For example, Manzo-Delgado *et al*. (2009) recorded distinct NDVI trends for grasslands, temperate, tropical forests and xerophytic scrubland in central Mexico and included vegetation type in their logistic model for predicting fire occurrence probability in their region of study.

DR values also showed sensitivity to the dryness between regions, with a consistent gradient from the more arid NW to the more humid S, present for most vegetation types. The NW region has a marked rain season starting in June-July, whereas in the tropical S precipitations are more constant throughout the year. Different timing of precipitation between regions likely drive the different patterns in the DR decrease, with an earlier start of this decrease for C and S regions, compared to a later decrease measured for most vegetation types in the NW region, probably caused by a later start of the rain season in this region in June-July.

Interestingly, the relationships between DR and FDI trends varied by vegetation type and region. For example, for many land uses such as agriculture, pasture or temperate forests, the increase of DR (upper lines, figure 2) occurred earlier in the NW region compared to a later occurrence of this DR increase in the central (C) or S regions. Looking at the FDI patterns for those land uses (figure 2, lower lines), the start of the fire season, as noted by an FDI increase, occurred earlier in C and S regions than in the NW, suggesting that either a longer accumulated drought is required in the NW region for fires to start, or human patterns of ignition might differ between these regions. These differences suggest that the relationships between DR trends and fire occurrence might be specific for each type of vegetation and region, as will be discussed in the section below.

Observed FDI trends by vegetation types and regions

The high FDI values observed in the S or C regions for agriculture and pasture are not surprising, because these territories are characterized by frequent slash-and burn agricultural activities and clearing forest for expansion of agriculture, which result in frequent fires (e.g. Rodriguez-Trejo and Fulé 2003; Román-Cuesta *et al*. 2004; Román-Cuesta and Martinez 2006; Rodríguez-Trejo *et al*. 2008, 2011; Carrillo *et al*. 2012; Ibarra-Montoya *et al*. 2016).

In the NW, the highest FDI values were observed for temperate forests, agreeing with previous studies in the region (e.g. Avila-Flores *et al*. 2010a, 2010b; Pérez-Verdin *et al*. 2011, 2013, 2014; Pompa-Garcia and Hernández Gonzalez 2016), who found that most of the fires in Durango State occurred on pine and oak temperate forest.

Lower FDI values were observed in the temperate forests of the NE region, which, as discussed above, is probably caused by higher precipitation in this region and an earlier DR decrease caused by an earlier start of the rain season compared to the NW. However, in years of extreme conditions such as 2011 under La Niña ENSO event, high fire occurrence was found in the forests of NE region, as noted by an FDI value of > 250 (> 5 fires /100 km^2) (figure 2). This extreme year corresponds to unprecedented area burnt, with the largest fire in Mexico's history - 317 000 ha -occurring in Northern Coahuila (CONAFOR, 2011).

There is no agreement in the literature about the role of El Niño/La Niña ENSO events in the NE region of Mexico (e.g. Yocom and Fulé,, 2012, Yocom *et al*. 2010, 2014), located at the transition between the areas affected by drought under the influence of El Niño (South) and those affected by La Niña (NW) (e.g. Román-Cuesta *et al*. 2003; Seager *et al*. 2007, 2009; Yocom *et al*. 2010). Meanwhile, the DR trends observed in 2011 for the NE region temperate forests, peaking at a value of 80 in April 2011, as opposed to DR values of less than 70, in most of the other years and corresponding with low FDI values of < 50 (figure 2), seem to suggest that extreme drought conditions were present in the NE forests under 2011 La Niña events. The extreme fire occurrence observed for that region for this period of time seems to suggest that DR might be a potentially useful indicator for detecting extreme fuel drought and associated fire risk conditions in this region caused by ENSO events, although a longer time frame will be required for assessing its performance under future El Niño/La Niña events.

Arboreous secondary vegetation showed high FDI values in the four regions, suggesting that this might be a fire-prone vegetation type. The likely cause being the high available fuel load that may be expected in these type of ecosystems, constituted by young trees with low crown height combined with high loads of surface fuels. Thus, providing a scenario of a potentially high risk of torching and potentially extreme fire behavior, as opposed to a lower risk of torching and lower severity fire regime expected in more mature forest types such as old-growth temperate forests (e.g. Morfin Ríos *et al*. 2007; Jardel *et al*. 2009, 2014; Cortés Montaño *et al*. 2012).

Perennial tropical forests (PTROPF) showed lower FDI values compared to deciduous tropical forests (DTROPF) in the NW, NE and S regions. This is expected in this evergreen ecosystem with high moisture conditions for most of the year, compared to drier conditions found in the DTROP, as noted by lower DR values in these latter ecosystems (figure 2). In the C region, both perennial and tropical forests showed high FDI values, in spite of lower DR values in PTROPF as expected in this more humid ecosystem. The high FDI values observed in this type of ecosystem with high moisture contents are very likely caused by adjacent agricultural burns escapes into forest lands. The majority of the perennial tropical forest area in this region can be found in the state of Chiapas, located in the vicinity of agricultural land (figure 1). In this state, reports of agricultural burns and escaped fires from agriculture to both temperate and perennial forest are frequent (e.g. Román-Cuesta et al., 2004; Román-Cuesta and Martinez 2006). Both deciduous and perennial tropical forests in Mexico have historically been ecosystems with a low frequency of fires (e.g. Rodríguez-Trejo *et al*. 2008, Jardel *et al*. 2014). However, several studies have noted that this historical fire regime has been recently reverted because of human activities that have resulted in the introduction of fire on ecosystems historically not adapted to it, with potentially adverse effects on post-fire regeneration of these fire-sensitive ecosystems (e.g. Rodríguez-Trejo 1996, 2008).

Models relating monthly FDI with DR by vegetation type and region

For all of the vegetation types and regions studied, the relationship of FDI with monthly DR was better described with nonlinear than with linear models, suggesting that the relationship of DR with fire occurrence is not linearly proportional –e.g. fire occurrence risk increases very rapidly with increasing DR. Different patterns of FDI and DR relationships were observed for different vegetation types and regions, agreeing with observations that point to a variety of fire regimes resulting from combinations of climatology and fuel types in the country (e.g. Rodríguez-Trejo 1996, 2008; Morfin Rios *et al*. 2007, 2012; Jardel *et al*. 2009, 2014).

The results suggested that significantly different models are required for prediction of FDI from DR for most vegetation types at different groups of months. Thus, derived model coefficients for months and groups of months may offer information about the patterns of timing of fire season and their relationships with DR patterns in different vegetation types and regions.

Models with grouped coefficients for December to February (eq. 22, 23 and 24, Table 1 and 2) suggest an earlier start of the fire season, with March having a higher coefficient value compared to the three previous months. This was observed for pasture (PAS) of all regions but NW, shrubby secondary vegetation (SHSV) from S and C, arboreous secondary vegetation (ARBSV) from C and NE, and TFOR of the NE. The timing of agricultural burning in C, S and NE regions might be behind this, with observed fires in SSHV and ARBSV starting as early as March being possibly related to escaped agricultural burns in these regions.

In the Central region, grouped coefficients from December to March were observed for temperate forest (TFOR) and deciduous- seasonally dry-tropical forest (DTROPF), (eq. 18, table 1), suggesting a latter start of fire at the month of April. For perennial tropical forests (PTFOR) in the Centre, grouped coefficients were obtained from December to April (eq. 16, table 1), suggesting that in this region, at least one more month of accumulated dry conditions might be required for fire to start in these more humid tropical forest ecosystems.

For the NW region, grouped coefficients from December to March were obtained for SHSV (eq. 21, Table 1) –one month later than S and C region-, with all the remaining vegetation types AG, ARBVS, TFOR, DTROPF and PTROPF, having grouped coefficients from December to April and separated coefficients for the month of May (eq. 16 and eq. 25), also suggesting a latter fire start for these vegetation types compared to other regions, particularly south and center.

These results seem to suggest that in the NW region, most vegetation types might be achieving the required conditions of accumulated drought for fire to occur one or two months later compared to other regions such as C or S, which might be linked to the different timing of precipitation between these regions, or to different patterns in the timing of human caused ignitions such as agricultural activities.

Most models had good fit, the exception being tropical forests models with a more limited performance. This is likely caused by a lower sensitivity of FDI to DR in this more humid ecosystems, where fires might spread from agricultural lands that are already dry and burnt under non-optimum conditions as discussed above. Several studies have pointed out at agricultural extension and the proximity to agricultural areas as significant factors explaining fire occurrence in tropical forests (e.g. Rodriguez-Trejo and Fulé 2003; Román-Cuesta and Martinez 2004, 2006; Rodríguez-Trejo *et al*. 2008, 2011). Future spatial analysis should focus on the integration of spatially explicit consideration of the interface of forests and agriculture as potentially relevant variables in explaining fire occurrence in this type of ecosystems where fire is progressively being introduced as a consequence of human activities. Another additional limitation of this first approach is the 12 year dataset utilized as defined by hotspots availability. This could be particularly limiting in a region such as the NE, where more data under extreme DR conditions (e.g. El Niño/La Niña events) might be required for a deeper understanding of drought and fire occurrence relationships.

Autoregressive integrated moving average (ARIMA) modeling of DR

DR could be successfully modeled with acceptable accuracies for most vegetation types by means of ARIMA, similar to works that have utilized these techniques for forecasting fire danger indices in other countries (e.g. Huesca et al., 2014).

It can be seen that tropical forests were among the models with a lower performance, perhaps due to the lower degree of variation observed in those more humid ecosystems.

DR underestimation occurred on some extreme peak years for some vegetation types. This could be caused by the limitations inherent to the time length of the dataset, limited by the 12 years of available satellite information, where only some years of extreme drought conditions are present. Continued monitoring of fire risk under varying fuel drought conditions might improve the ability of these initial models to account for extreme events. In addition, a joint consideration of ENSO indices might help improve forecast of extreme drought events and associated fire risk.

Future work will focus on exploring indices that integrate satellite information with weather-based fuel greenness indices at finer temporal resolutions (e.g. Burgan *et al*. 1998) together with exploring the potential of weather forecasts for fire risk forecasting (e.g. Roads *et al*. 2003, 2005).

CONCLUSIONS

The current study represents substantial progress toward developing a system for prediction of fire occurrence risk based on temporal trends in fire density and fuel drought. Temporal trends were measured by a satellite relative greenness index, DR, in different types of vegetation and regions in Mexico, at a national scale, with a monthly temporal resolution, for the period 2003-2014. DR trends varied by vegetation type and region, with drier fuel conditions measured in the most arid type of fuels and regions. Furthermore, significant relationships were found relating monthly fire density and DR for the analyzed vegetation types and regions in the period of study. In addition, we obtained preliminary seasonal autorregresive integrated moving average models for prediction of monthly DR values which might be incorporated into future fire risk forecast operational tools. Whereas these initial results suggest the potential of the indices utilized for capturing both short-term and long-term drought phenomena and its impact on fire occurrence in the country, a longer time period of monitoring will be required for improving our understanding of long-term climatic effects, such as El Niño/La Niña impact on fuel drought and associated fire risk in the country.

Future work, in the frame of the CONAFOR/CONACYT project for the development of an operational fire danger system in Mexico will explore temporal trends of fire occurrence with satellite and weather based indices of fuel greenness at finer temporal resolutions. Our future studies within this project will also focus on the consideration of the spatial patterns of fire density as related to weather, fuels and human factors (e.g. distance to roads, population, agriculture) for a further understanding of the spatial-temporal patterns of fire in Mexico.

ACKNOWLEDGEMENTS

Funding for this work was provided by CONAFOR/CONACYT Project C0-3-2014 “Development of a Fire Danger System for Mexico”. This work was also co-financed by the INIA and European Social Fund (Dr. E. Jiménez grant). We want to thank CONABIO’s personnel for providing us access to the MODIS hot spots data for Mexico for the period of study.

LITERATURE CITED

Antonio, X. and E.A. Ellis. 2015. Forest Fires and Climate Correlation in México State: A Report Based on MODIS. Advances in Remote Sensing 4: 280-286.

Avila-Flores, D., M. Pompa-García, and E. Vargas-Pérez. 2010a. Spatial analysis of fire occurrence in the Durango State. Revista Chapingo. Serie Ciencias Forestales 16(2): 253–260.

Avila-Flores, D., M. Pompa-García, X. Antonio-Nemiga, D.A. Rodríguez-Trejo, E. Vargas-Perez, and J. Santillan-Pérez. 2010b. Driving factors for forest fire occurrence in Durango State of México: a geospatial perspective. Chinese Geographical Science 20: 491–497.

Bates, D.M. and Watts, D.G. 1988 Nonlinear regression analysis and its applications. John Wiley & Sons, New York.

Burgan, R.E., and R.A. Hartford. 1993. Monitoring vegetation greenness with satellite data. United States Department of Agriculture, Forest Service, General Technical Report INT-297, Intermountain Forest and Range Experiment Station, Ogden, Utah.

Burgan, R.E., and R.A. Hartford. 1997. Live vegetation moisture calculated from NDVI and used in fire danger rating. 13th Conf. on Fire and For. Met., Lorne, Australia, Oct. 27-31, 1997. Jason Greenlee, ed. IAWF, Fairfield, WA 99012.

Burgan, R.E., P.L. Andrews, L.S. Bradshaw, C.H. Chase, R.A. Hartford, and D.J. Latham. 1997. WFAS: wildland fire assessment system, Fire Management Notes 57(2): 14-17.

Burgan, R.E., R.A. Hartford, and J.C. Eidenshink. 1996. Using NDVI to assess departure from average greenness and its relation to fire business. Gen. Tech. Rep. INT-GTR-333. Ogden, UT:U.S. Department of Agriculture, Forest Service, Intermountain Research Station.

Burgan, R.E., R.W. Klaver, and J.M. Klaver. 1998. Fuel Models and Fire Potential from Satellite and Surface Observations. International Journal of Wildland Fire 8(3): 159-170.

Carrillo García R.L., D.A. Rodríguez Trejo, H. Tchikoué, A.I. Monterroso Rivas, and J. Santillan Pérez. 2012. Análisis espacial de peligro de incendios forestales en Puebla, México. Interciencia 37(9): 678-683

Castañeda Rojas, M.F., A.R. Endara Agramont, M.L. Villers Ruiz, and G. Nava Bernal. 2015. Evaluación forestal y de combustibles en bosques de *Pinus hartwegii* en el Estado de México según densidades de cobertura y vulnerabilidad a incendios. Madera y bosques 21(2): 45-58.

Castedo, F., Barrio, M., Parresol, B.R. and Álvarez González, J.G. 2005 A stochastic height-diameter model for maritime pine ecoregions in Galicia (northwestern Spain). Ann. For. Sci. 62: 455-465.

Cerano Paredes J., J. Villanueva Díaz, and P.Z. Fulé. 2010. Reconstrucción de incendios y su relación con el clima para la reserva Cerro el Mohinora, Chihuahua. Revista Mexicana de Ciencias Forestales 1(1): 64-76.

Chuvieco, E., I. Aguado, and P. Dimitrakopoulos. 2004. Conversion of fuel moisture content values to ignition potential for integrated fire danger assessment. Canadian Journal of Forest Research 34: 2284–2293.

Chuvieco, E., I. Aguado, M. Yebra, H. Nieto, J. Salas, M.P. Martín, L. Vilar, J. Martínez, S. Martín, P. Ibarra, J. de la Riva, J. Baeza, F. Rodríguez, J.R. Molina, M.A. Herrera, and R. Zamora. 2010. Development of a framework for fire risk assessment using remote sensing and geographic information system technologies. Ecological Modelling 221: 46-58.

CONAFOR. Comisión Nacional Forestal. 2011. Evaluación preliminar de incendios en La Sabina y El Bonito, municipios de Múzquiz, Ocampo, Zaragoza y Acuña, del estado de Coahuila. Informe ejecutivo. Conafor, Semarnat. Zapopan, Jalisco.

Cortés Montaño C., P.Z. Fulé, D.A. Falk, J. Villanueva-Díaz, and L.L. Yocom. 2012. Linking old-growth forest composition, structure, fire history, climate and land-use in the mountains of northern México. Ecosphere 3(11): 1-16.

Corral-Rivas, J.J., Álvarez González, J.G., Ruiz, A.D. and Gadow, K.v. 2004 Compatible height and site index models for five pine species in El Salto, Durango (Mexico). For. Ecol. Manage. 201: 145–160.

Corral-Rivas J.J., Barrio Anta M., Treviño Garza E., Diéguez-Aranda U. 2007. Use of stump diameter to estimate diameter at breast height and tree volume, for major pine species in El Salto, Durango (Mexico). Forestry 80(1):29-40

Deeming, J.E., R.E. Burgan, and J.D. Cohen. 1977. The National Fire-Danger Rating System - 1978. Gen. Tech. Rep. INT-39. Ogden, UT: U.S. Department of Agriculture, Forest Service, Intermountain Forest and Range Experiment Station.

Drury, S.A. and T.T. Veblen. 2008. Spatial and temporal variability in fire occurrence within the Las Bayas Forestry Reserve, Durango, México. Plant. Ecology 197: 299-316.

ESRI 2011. ArcGIS Desktop: Release 10. Redlands, CA: Environmental Systems Research Institute.

Fernández-Manso, A., C. Quintano, and O. Fernández-Manso. 2011. Forecast of NDVI in coniferous areas using temporal ARIMA analysis and climatic data at a regional scale. International Journal of Remote Sensing 32: 1595–1617.

Flannigan, M.D., B.D. Amiro, K.A. Logan, B.J. Stocks, and B.M. Wotton. 2006. Forest fires and climate change in the 21st century. Mitigation and adaptation strategies for global change 11(4): 847-859.

Flannigan M, B. Stocks, M. Turetsky, and M. Wotton. 2009. Impacts of climate change on fire activity and fire management in the circumboreal forest. Global Change Biology 15: 549–60.

Flores Garnica J.G., J.D. Benavides Solorio, and A. Martinez Moreno. 1990. Índices de riesgos de incendio en la sierra de Tapalpa, estado de Jalisco. Revista Ciencia Forestal en México 67(15): 4-34.

Fosberg, M.A., and J.E. Deeming. 1971. Derivation of the 1- and 10-hour timelag fuel moisture calculations for fire-danger rating. USDA Forest Service Research Note RM-207, Ft. Collins, CO.

Fulé, P.Z., J. Villanueva-Díaz, and M. Ramos-Gómez. 2005. Fire regime in a conservation reserve in Chihuahua, México. NRC. Canadian Journal of Forest Research 35: 320-330.

Gillett N.P., A.J. Weaver, F.W. Zwiers, and M.D. Flannigan. 2004. Detecting the effect of climate change on Canadian forest fires. Geophysical Research Letters 31: L18211

González-Cabán, A. and D.V. Sandberg. 1989. Fire management and research needs in México. Journal of Forestry 87: 20-26.

Hamilton, J.D. 1994. Time Series Analysis. Princeton University Press, Princeton.

Heyerdahl, E.K. and E. Alvarado. 2003. Influence of climate and land use on historical surface fires in pine-oak forests, Sierra Madre Occidental, Mexico. In: T.T. Veblen, W.L. Baker, G. Montenegro and T.W. Swetnam. Eds. Fire and climatic change in temperate ecosystems of the Western Americas. Springer Verlag. New York, NY. USA. pp. 196-217.

Holridge L. 1996. Ecología basada en Zonas de Vida. Instituto Interamericano de Cooperación para la Agricultura. San José.

Huang, S., Price, D. and Titus, S.J. 2000a Development of ecoregion-based height-diameter models for white spruce in boreal forests. For. Ecol. Manage. 129: 125–141.

Huesca, M., J. Litago, A. Palacios-Orueta, F. Montes, A. Sebastián-López, and P. Escribano. 2009. Assessment of forest fire seasonality using MODIS fire potential: a timeseries approach. Agricultural and Forest Meteorology 149: 1946–1955.

Huesca, M., J. Litago, S. Merino-de-Miguel, V. Cicuendez-López-Ocaña, and A. Palacios-Orueta. 2014. Modeling and forecasting MODIS-based Fire Potential Index on a pixel basis using time series models. International Journal of Applied Earth Observation and Geoinformation 26: 363–376

Huesca, M., A. Palacios-Orueta, F. Montes, A. Sebastián-López, and P. Escribano. 2007. Forest Fire Potential Index for Navarra Autonomic Community (Spain). In: Wildland Fire International Conference. Seville 2007.

Hyndman, R. 2016. Package 'forecast'. R Package Documentation, github: CRAN Repository.

Ibarra-Montoya J.L., and F.M. Huerta-Martínez. 2016. Modelado espacial de incendios: una herramienta predictiva para el Bosque La Primavera, Jalisco México. Ambiente & Agua 11(1): 36-51.

Jardel, E.J., E. Alvarado, J.E. Morfín-Ríos, F. Castillo-Navarro, and J.G. Flores-Garnica. 2009. Regímenes de incendios en ecosistemas forestales de México. En: J.G. Flores-Garnica. Ed. Impacto Ambiental de Incendios Forestales. Mundi-Prensa, INIFAP y Colegio de Postgraduados. México D.F.

Jardel, E.J., D. Pérez-Salicrup, E. Alvarado, and J.E. Morfín Ríos. 2014. Principios y criterios para el manejo del fuego en ecosistemas forestales: guía de campo. Comisión Nacional Forestal. Guadalajara, Jalisco, México.

López A.S., J. San-Miguel-Ayanz, and R.E. Burgan. 2002. Integration of satellite sensor data, fuel type maps and meteorological observations for evaluations of forest fire risk at the pan-European scale. International Journal of Remote Sensing 23(13): 2713-2719.

Lozano, F.J., S. Suárez-Seoane, and E. De Luis. 2007. Assessment of several spectral indices derived from multi-temporal Landsat data for fire occurrence probability modelling. Remote Sensing of Environment 107: 533-544.

Lozano, F.J., S. Suarez-Seoane, and E. De Luis. 2008. A multi-scale approach for modeling fire occurrence probability using satellite data and classification trees: a case study in a mountainous Mediterranean region. Remote Sensing of Environment 112 (3): 708–719.

Manzo-Delgado, L., R. Aguirre-Gómez, and R. Álvarez. 2004. Multitemporal analysis of land surface temperature using NOAA-AVHRR: preliminary relationships between climatic anomalies and forest fires. International Journal of Remote Sensing 25: 4417–4423.

Manzo-Delgado, L. S. Sánchez-Colón, and R. Álvarez. 2009. Assessment of seasonal forest fire risk using NOAA-AVHRR: a case study in central Mexico. International Journal of Remote Sensing 30(19): 4991-5013

Mavsar, R., A. González-Cabán, and E. Varela. 2013. The State of Development of Fire Management Decision Support Systems in America and Europe. Forest Policy and Economics 29: 45–55

Morfín Ríos, J.E., E. Alvarado Celestino, E.J. Jardel Peláez, R.E. Vihnanek, D.K. Wright, J.M. Michel Fuentes, C.S. Wright, R.D. Ottmar, D.V. Sandberg, and A. Nájera Díaz. 2007. Fotoseries para la Cuantificación de Combustibles Forestales de México: Bosques Montanos Subtropicales de la Sierra Madre del Sur y Bosques Templados y Matorral Submontano del Norte de la Sierra Madre Oriental. Gen. Tech. Rep. PNW-GTR-XXX. Portland, OR: U.S. Department of Agriculture, Forest Service, Pacific Northwest Research Station.

Morfin Rios, J.E., E.J. Jardel Peláez, and J.M. Michel Fuentes. 2012. Caracterización y cuantificación de combustibles forestales. Comisión Nacional Forestal. Universidad de Guadalajara, Guadalajara, Jalisco, México.

Muñoz Robles C.A., E.J. Treviño Garza, J. Verástegui Chávez, J. Jiménez Pérez, and O.A. Aguirre Calderón. 2005. Desarrollo de un modelo espacial para la evaluación del peligro de incendios forestales en la sierra madre oriental de México. Investigaciones Geográficas 56: 101-117.

Návar-Cháidez J.J., and L.G. Lizárraga-Mendiola. 2013. Hydro-climatic variability and forest fires in Mexico's northern temperate forests. Geofísica Internacional 52: 5–20.

Pérez-Verdin G., M.A. Márquez-Linares, A. Cortes-Ortiz, and M. Salmerón-Macias. 2011. Patrones de Distribución Espacio Temporal de los Incendios Forestales en el Norte de México. Memorias del Cuarto Simposio Internacional Sobre Políticas, Planificación y Economía de los Incendios Forestales: Cambio Climático e Incendios Forestales

Pérez-Verdín, G., M.A. Márquez-Linares, A. Cortés-Ortiz, and M. Salmerón-Macías. 2013. Análisis espacio-temporal de la ocurrencia de incendios forestales en Durango, México. Madera y bosques 19(2): 37-58.

Perez-Verdin G., M.A. Marquez-Linares, and M. Salmeron-Macias. 2014. Spatial heterogeneity of factors influencing forest fires size in northern Mèxico. Journal of Forestry Research 25(2): 291−300.

Pompa-García M., and P. Hernández González. 2016. Determinación de la tendencia espacial de los puntos de calor como estrategia para monitorear los incendios forestales en Durango, México.. Bosque 33(1): 63-68, 2012

Preisler, H.K., and A.L. Westerling. 2007. Statistical model for forecasting monthly large wildfire events in western United States. Journal of Applied Meteorology and Climatology 46: 1020–1030.

Preisler, H.K., D. Brillinger, R.E. Burgan, and J.W. Benoit. 2004. Probability based models for estimation of wildfire risk. International Journal of Wildland Fire 13: 133–142.

Preisler, H.K., R.E. Burgan, J.C. Eidenshink, J.M. Klaver, and R.W. Klaver. 2009. Forecasting Distributions Of Large Federal-Lands Fires Utilizing Satellite And Gridded Weather Information. International Journal of Wildland Fire 18: 508–516

Preisler, H.K., S.C. Chen, F. Fujioka, J.W. Benoit, and A.L. Westerling. 2008. Wildland fire probabilities estimated from weather model-deduced monthly mean fire danger indices. International Journal of Wildland Fire 17 305–316.

Preisler, H.K., J.C. Eidenshink, S. Howard, and R.E Burgan. 2015. Forecasting Distribution of Numbers of Large Fires. USDA Forest Service Proceedings RMRS-P-73.

Preisler, H.K., A.L. Westerling, K.M. Gebert, F. Munoz-Arriola, and T.P. Holmes. 2011. Spatially explicit forecasts of large wildland fire probability and suppression costs for California. International Journal of Wild land Fire 20: 508–517.

R Core Team. 2016. R: A language and environment for statistical computing. R Fpundation for Statistical Computing, Vienna, Austria. (http//www.R-project.org/)

Riley K.L., J.T. Abatzoglou, I.C. Grenfell, A.E. Klene, and F.A. Heinsch. 2013. The relationship of large fire occurrence with drought and fire danger indices in the western USA, 1984–2008: the role of temporal scale. International Journal of Wildland Fire 22: 894–909.

Roads, J.O., S.C. Chen, and M. Kanamitsu. 2003. US regional climate simulations and seasonal forecasts. Journal of Geophysical Research 108: 8606.

Roads, J.O., F. Fujioka, S.C. Chen and R.E. Burgan. 2005. Seasonal fire danger forecasts for the USA. International Journal of Wildland Fire 14: 1-18.

Rodríguez y Silva, F., J.R. Molina Martínez, and A. González-Cabán. 2014. A Methodology for Determining Operational Priorities for Prevention and Suppression of Wildland Fires. International Journal of Wildland Fire 24(3): 544-554

Rodriguez-Trejo, D.A. 1996. Incendios forestales. Universidad Autónoma Chapingo. Multi-Prensa. Mexico.

Rodríguez-Trejo, D.A. 2008. Fire regimes, fire ecology and fire management in México. AMBIO: A Journal of the Human Environment 37(7): 548-556.

Rodríguez-Trejo, D.A., and P.Z. Fulé. 2003. Fire ecology of Mexican pines and fire management proposal. International Journal of Wildlife Fire 12:23-37

Rodríguez-Trejo, D.A., H. Ramírez, H. Tchikoué, and J. Santillán. 2008. Factores que inciden en la siniestralidad de los incendios forestales. Ciencia Forestal 33: 37-58.

Rodríguez-Trejo, D.A., H. Tchikoué, C. Cíntora, R. Contreras, and A. de la Rosa. 2011. Combustibles forestales, peligro de incendio y áreas prioritarias de protección en las zonas afectadas por el huracán Dean. Agrociencia 45: 593-608.

Román-Cuesta, R.M., and J.V. Martínez. 2006. Effectiveness of protected areas in mitigating fire within their boundaries: case study of Chiapas, México. Conservation Biology 20 (4): 1074-1086.

Román-Cuesta, R.M., M. Gracia and J. Retana. 2003. Environmental and human factors influencing fire trends in ENSO and non-ENSO years in tropical Mexico. Ecological Applications 13(4):1177-1192.

Román-Cuesta, R.M., J. Retana, and M. Gracia. 2004. Fire trends in tropical Mexico: a case study of Chiapas. Journal of Forestry 102:26–48.

SAS Institute Inc. 2009. Base SAS® 9.2 procedures guide. SAS Institute Inc., Cary, NC.

Seager, R., M. Ting, M. Davis, M. Cane, N. Naik, J. Nakamura, C. Li, E. Cook, and D.W. Stahle. 2009. Mexican drought: an observational modeling and tree ring study of variability and climate change. Atmosfera 22:1–31.

Seager, R., M. Ting, I. Held, Y. Kushnir, J. Lu, G. Vecchi, H.P. Huang, N. Harnik, A. Leetmaa, N.C. Lau, C. Li, J. Velez, and N. Naik. 2007. Model projections of an imminent transition to a more arid climate in southwestern North America. Science 316:1181–1184

Sebastian-Lopez, A., J. San-Miguel-Ayanz, and R.E. Burgan. 2002. Integration of satellite sensor data, fuel type maps and meteorological observations for evaluation of forest fire risk at the pan-European scale. International Journal of Remote Sensing 23(13): 2713–2719.

Sepúlveda, B.J., R. Meza, C.W. Zúñiga, G. Solìs, and E.M. Olguín. 2001. SIG para determinar riesgo de incendios forestales en el noroeste de Mexico. INIFAP, SAGAR, México.

Sepúlveda, B.J., C.W. Zúñiga, E.M. Olguín and P.A. Gomero. 1999. Implementación de un sistema de información geográfica para la prevención de incendios forestales en Baja California, Folleto Científico No. 1, INIFAP, SAGAR, México.

Setzer, A.W., and R.A. Sismanoglu. 2012. Risco de Fogo: Metodologia do Cálculo – Descrição sucinta da Versão 9 .INPE Report.

Skinner, C.N., J.H. Burk, M.G. Barbourt, E. Franco-Vizcaíno, and S.L. Stephens. 2008. Influences of climate on fire regimes in montane forests of north-western Mexico. Journal of Biogeography 35: 1436-1451.

Van Wagner C.E., 1987. Development and structure of the Canadian Forest Fire Weather Index System. Canadian Forestry Service, Forestry Technical Report 35. Ottawa, Canada.

Villers-Ruiz M.L., E. Chuvieco, and I. Aguado. 2012. Aplicación del Índice Meteorológico de Incendios Canadiense en un Parque Nacional del centro de México. Revista Mexicana de Ciencias Forestales 3(11): 25-40.

Vega-Nieva D., P.M. Lopez-Serrano, J. Briseño-Reyes, C.A. Lopez-Sanchez, J.J. Corral-Rivas, C. Cortes-Montaño, E. Alvarado-Celestino, A. Gonzalez-Caban, A. Setzer, I. Cruz, R. Ressl, D. Perez-Salicrup, M.L. Villers-Ruiz, L.M. Morales-Manilla, E. Jardel-Pelaez, J.A. Vega, and E. Jiménez. 2015. Development of an operational Fire Danger System for Mexico. In: Fire Ecology & Management Congress. Advancing Ecology in Fire Management, At San Antonio, Texas, USA.

Wong González J.C., and M.L. Villers Ruiz. 2007. Evaluación de combustibles y su disponibilidad en incendios forestales: un estudio en el Parque Nacional La Malinche. Investigaciones Geográficas 62: 87-103.

Woolford, D.G., C.B. Dean, D.L. Martell, J. Cao, J. and B.M. Wotton. 2013. Lightning-caused forest fire risk in Northwestern Ontario, Canada is increasing and associated with anomalies in fire-weather. Environmetrics 25(6): 406-416.

Wotton, B.M, Martell, D.L., and K.A. Logan. 2003. Climate change and human caused forest fire occurrence in Ontario. Climatic Change 60: 275–295.

Yebra, M., E. Chuvieco, and D. Riaño. 2008. Estimation of live fuel moisture content from MODIS images for fire risk assessment. Agricultural and Forest Meteorology 148: 523-536.

Yebra, M., P.E. Dennison, E. Chuvieco, D. Riaño, P. Zylstra, R. Hunt, F.M. Danson, Y. Qi, and S. Jurdao. 2013. A global review of remote sensing of live fuel moisture content for fire danger assessment: Moving towards operational products. Remote Sensing of Environment 136: 455–468|

Yocom, L.L., and P.Z. Fulè. 2012. Human and climate influences on frequent fire in a high-elevation tropical forest. Journal of Applied Ecology 49 (6): 1356-1364

Yocom, L.L., P.Z. Fulè, P.M. Brown, J. Cerano-Paredes, J. Villanueva, E. Cornejo Oviedo, and D.A. Falk. 2010. El Nino–Southern Oscillation effect on a fire regime in northeastern Mexico has changed over time. Ecology 91, 1660–1671.

Yocom, L.L., P.Z. Fulè, D. Falk, C. Garcia-Dominguez, E. Cornejo-Oviedo, P.M. Brown, J. Villanueva-Díaz, J. Cerano, and C. Cortés Montaño. 2014. Fine-scale factors influence fire regimes in mixed-conifer forests on three high mountains in México. International Journal of Wildland Fire 23(7): 959-968.

Zhang, L., Peng, L., Huang, S. and Zhou, X. 2002 Development and evaluation of ecoregion-based tree height-diameter models for jack pine in Ontario, For. Chron. 78, 530-538.

TABLES

Veg	Eq. n	Grouped months	Equation
All but AG	7	All months grouped	$FDI = aDR^{b}$
	16	12-4&6, 5	$FDI = (d_{12-4\&6}a_{12-4\&6}DR + d_{5}a_{5}DR)^{b}$
	17	12-3, 4-6	$FDI = (d_{12-3}a_{12-3}DR + d_{4-6}a_{4-6}DR)^{b}$
	18	12-3, 4&6, 5	$FDI = (d_{12-3}a_{12-3}DR + d_{4\&6}a_{4\&6}DR + d_{5}a_{5}DR)^{b}$
	19	12-3, 4&5, 6	$FDI = (d_{12-3}a_{12-3}DR + d_{4\&5}a_{4\&5}DR + d_{6}a_{6}DR)^{b}$
	20	12-3&6, 4&5	$FDI = (d_{12-3\&6}a_{12-3\&6}DR + d_{4\&5}a_{4\&5}DR)^{b}$
	21	12-3&6, 4, 5	$FDI = (d_{12-3\&6}a_{12-3\&6}DR + d_{4}a_{4}DR + d_{5}a_{5}DR)^{b}$
	22	12-2, 3, 4&6, 5	$FDI = (d_{12-2}a_{12-2}DR + d_{3}a_{3}DR + d_{4\&6}a_{4\&6}DR + d_{5}a_{5}DR)^{b}$
	23	12-2, 3&6, 4, 5	$FDI = (d_{12-2}a_{12-2}DR + d_{3\&6}a_{3\&6}DR + d_{4}a_{4}DR + d_{5}a_{5}DR)^{b}$
	24	12-2&6, 3, 4&5	$FDI = (d_{12-2\&6}a_{12-2\&6}DR + d_{3}a_{3}DR + d_{4\&5}a_{4\&5}DR)^{b}$
AG	25	9-4, 5-8	$FDI = (d_{9-4}a_{9-4}DR + d_{5-8}a_{5-8}DR)^{b}$
	26	9-3, 4-6, 7&8	$FDI = (d_{9-3}a_{9-3}DR + d_{4-6}a_{4-6}DR + d_{7\&8}a_{7\&8}DR)^{b}$
	27	9-3&7&8,4, 5&6	$FDI = (d_{9-3\&7-8}a_{9-3\&7-8}DR + d_{4}a_{4}DR_{4} + d_{5\&6}a_{5\&6}DR_{5\&6})^{b}$

Table 1. Selected models for prediction of monthly Fire Density Index from Dead Ratio values. Where: Veg: Vegetation type; AG: Agriculture; All but AG: All vegetation types except agriculture; Eq. N: number of equation; FDI: monthly Fire Density Index, DR: monthly Dead Ratio, *a* and *b* are model coefficients, d_i: Dummy variable for identifying month or group of months "i", with value =1 for the identified month or group of months "i" and value =0 for the remaining months. Numbers in coefficients and in model description correspond to months or groups of months, with 12: December, 1: January, 2: February, 3: March, 4: April, 5: May, 6: June, 7: July, 8: August, 9: September, 10: October, 11: November.

Veg_region	Eq	a	a12-2	a12-2&6	a12-3	a12-3&6	a12-4&6	a3	a3&6	a4	a4&5	a4-6	a4&6	a5	a6	a5&6	a7&8	a5-8	a9-3	a9-4	a9-3 &7-8	b	rho	RMSE	R^2_{adj}	AIC
TFOR_C	18				0.0194								0.022	0.02								9.2629	0.535	27.3	0.82	563
TFOR_NE	22		0.0161					0.02					0.02	0.02								9.1414	0.394	13.3	0.69	442
TFOR_NW	16						0.018							0.02								8.0916	1.479	26.5	0.72	556
TFOR_S	19				0.0161						0.015				0.01							26.057	0.321	10.5	0.71	403
PAS_C	22		0.0191					0.02					0.027	0.03								5.4058	0.398	15.6	0.96	470
PAS_NE	22		0.0195					0.02					0.024	0.03								5.5583	0.402	8	0.89	357
PAS_NW	7	0.01																				20.634	1.227	3	0.64	88
PAS_S	23		0.0528						0.102	0.18				0.2								2.2174	0.326	81.9	0.82	748
PTROPF_C	16						0.0248							0.03								6.8375	0.097	36.2	0.77	609
PTROPF_NE	21					0.0377				0.07				0.08								2.9451	0.164	17.8	0.68	490
PTROPF_NW	16						0.0212							0.03								3.3332	0.301	7.6	0.74	347
PTROPF_S	18				0.02								0.023	0.03								7.004	0.417	6.4	0.75	319
DTROPF_C	18				0.0229								0.048	0.05								3.234	0.237	17.7	0.92	489
DTROPF_NE	16						0.0412							0.05								3.9978	1.14	58.1	0.68	688
DTROPF_NW	16						0.0151							0.02								7.7482	0.892	10.6	0.86	402
DTROPF_S	7	0.03																				5.5697	0.326	30.2	0.7	255
ARBVS_C	23		0.0193						0.024	0.03				0.03								5.688	0.403	22.9	0.92	534
ARBVS_NE	22		0.0218					0.03					0.028	0.03								6.0022	0.174	9.7	0.94	390
ARBVS_NW	16						0.0208							0.02								5.8133	0.582	26.4	0.72	556
ARBVS_S	24			0.034				0.06			0.088											2.8021	0.287	32.8	0.82	264
SHVS_C	22		0.0165					0.02					0.024	0.03								6.1675	0.619	14.4	0.95	456
SHVS_NE	20					0.0176					0.022											7.1694	0.35	13.1	0.76	196
SHVS_NW	21					0.0123				0.02				0.02								5.8976	1.991	12.2	0.84	192
SHVS_S	23		0.0302						0.044	0.06				0.06								3.7905	0.244	54.8	0.8	680
AG_S	27									0.07						0.064					0.0544	3.4732	1.616	62.2	0.79	1196
AG_NW	25																	0.041		0.031		3.1607	0.821	11.6	0.7	711
AG_NE	26											0.023					0.019		0.021			5.6447	0.856	5	0.79	471
AG_C	27									0.02						0.022					0.0190	6.68	0.156	8.8	0.86	635

Table 2. Coefficients and goodness of fit of the best fit equations for the prediction of monthly Fire Density Index from Dead Ratio values for each vegetation type and region. Where: Veg_Reg: Vegetation and region; Eq: best fit equation from table 1; *a, b* and *rho* are global parameters; *a1 to a12* are parameters associated to the corresponding months (January to December) or group of months; RMSE: Root Mean Square Error; R^2adj: Adjusted R^2; AIC: Standard AIC; AG: Agriculture; ARBSV: Arboreous Secondary Vegetation, DTROPF: Deciduous Tropical Forest, PAS: Pastureland, PTROPF: Perennial Tropical Forest, SHSV: Shrubby Secondary Vegetation, TFOR: Temperate Forest and NW: NWrth West, NE: NWrth East, C: Centre, S: South regions.

Veg_region	ARIMA	ar1	ar2	ar3	ar4	ar5	ar6	ma1	ma2	sar1	sar2	sar3	sar4	sma1	sma2	sma3	intercept	R^2 adj	RMSE	AIC
AG_C	(2,0,1) x(0,0,2)	1.623	-0.87					-0.674						0.3246	0.5201		71.2447	0.86	18.8	857
AG_NE	(1,0,1) x(2,0,0)	0.6421						0.3577		0.4178	0.3305						67.9347	0.74	11.6	780.8
AG_NW	(6,0,2) x(0,0,3)	-0.593	0.3134	0.3828	-0.451	-0.206	0.089	1.6016	1					0.6511	0.7743	0.5639	78.5641	0.83	8.9	771
AG_S	(2,0,1) x(2,0,0)	1.4888	-0.667					-0.689		0.2634	0.4055						54.7732	0.70	29.2	912.6
ARBSV_C	(2,0,2) x(0,0,2)	1.6727	-0.932					-0.984	0.2711					0.1872	0.555		58.8577	0.84	16.2	835
ARBSV_NE	(5,0,1) x(1,0,0)	1.2508	-0.581	-0.075	0.171	-0.302		-0.214		0.1314							53.7640	0.77	7.1	710.4
ARBSV_NW	(3,0,0) x(2,0,0)	0.6589	-0.015	0.076						0.2471	0.7095						69.0646	0.89	15.1	842.5
ARBSV_S	(3,0,0) x(2,0,0)	0.7507	-0.195	0.0099						0.3245	0.4445						49.0004	0.66	22.7	879.7
DTROPF_C	(5,0,1) x(2,0,3)	0.0683	0.1381	-0.093	-0.017	0.0863		0.3664		0.0003	0.995			0.2855	-0.758	-0.08	65.1418	0.90	23.9	927
DTROPF_NE	(2,0,0) x(2,0,0)	1.0509	-0.347							0.3229	0.3404						57.3068	0.72	27.1	900.2
DTROPF_NW	(2,0,0) x(2,0,0)	0.5344	0.0891							0.2382	0.7093						66.8218	0.85	36.9	967.7
DTROPF_S	(2,0,1) x(2,0,0)	1.5354	-0.689					-0.854		0.3504	0.3615						51.024	0.70	14.9	816.1
PAS_C	(2,0,1) x(0,0,2)	1.6455	-0.891					-0.697						0.2478	0.492		66.9155	0.86	20.6	864.9
PAS_NE	(1,0,0) x(2,0,0)	0.728								0.3816	0.3828						64.2352	0.65	16.2	827.2
PAS_NW	(2,0,1) x(0,0,2)	1.5273	-0.771					-0.594						0.535	0.5502		82.9653	0.79	16.7	836.4
PAS_S	(2,0,0) x(2,0,0)	0.7707	-0.172							0.3609	0.4003						54.1157	0.67	32.8	930.7
PTROPF_C	(5,0,2) x(0,0,2)	2.216	-2.051	0.7989	-0.12	-0.054		-1.718	0.9993					0.2919	0.4685		53.2126	0.86	11.9	795.5
PTROPF_NE	(5,0,1) x(1,0,1)	1.0465	-0.316	0.0754	0.0432	-0.11		-0.662		0.9999				-0.985			46.8883	0.64	3.6	641.9
PTROPF_NW	(3,0,2) x(1,0,2)	0.1458	-0.672	0.5883				0.4425	1	0.9889				-1.135	0.5149		58.4015	0.88	26.4	936.6
PTROPF_S	(1,0,1) x(2,0,0)	0.3176						0.4732		0.3801	0.3366						49.1263	0.60	13.3	798.8
SHSV_C	(2,0,1) x(0,0,2)	1.6326	-0.875					-0.68						0.2324	0.568		66.1444	0.84	21.1	870.7
SHSV_NE	(4,0,1) x(4,0,0)	1.3012	-0.637	0.3147	-0.215			-0.201		0.2713	0.1131	0.314	0.021				67.2066	0.79	10.8	774.4
SHSV_NW	(2,0,1) x(0,0,2)	1.5459	-0.79					-0.561						0.4084	0.58		78.6086	0.81	16.5	834.8
SHSV_S	(2,0,1) x(2,0,0)	1.5005	-0.67					-0.735		0.2529	0.4262						52.1467	0.68	23.3	880.2
TFOR_C	(3,0,2) x(3,0,2)	1.5236	-1.551	0.6111				-0.957	1	-0.076	0.6902	0.372		0.0685	-0.356		58.2776	0.90	6.5	734.5
TFOR_NE	(1,0,1) x(2,0,0)	0.6455						0.501		0.357	0.3603						58.7626	0.77	9.4	749.6
TFOR_NW	(6,0,2) x(1,0,2)	0.719	0.3792	-0.301	0.0216	-0.051	0.05	0.0289	-0.411	0.9877				-0.563	-0.061		70.5062	0.90	8.4	765
TFOR_S	(1,0,0) x(1,0,0)	0.6886								0.7728							61.1325	0.74	7.9	725

Table 3. Coefficients and goodness of fit of the best fit seasonal ARIMA models for prediction of DR. Where: Veg_Reg: Vegetation and region; ARIMA: Best fit ARIMA models of order (*ar.dif,ma*) x(*sar,sdif,sma*)S, where *ar* is the autorregresive order, *dif*: is the integrated order, *ma* is the mean average order, *sar, sdif* and *sma* are the seasonal autorregresive, integrated and mean average order, respectively and *S* = time span of repeating seasonal pattern (12 months); $ar_{i=}$ autorregresive coefficients of the order *i*, ma_i= are moving average coefficients of the order *i*, sar_i are seasonal autorregresive coefficients, of the order *i*, sma_i are seasonal moving average coefficients of the order *i*, *intercept:* seasonal ARIMA model intercept; R^2adj: Adjusted R^2; RMSE: Root Mean Square Error; AIC: Standard AIC; AG: Agriculture; ARBSV: Arboreous Secondary Vegetation, DTROPF: Deciduous Tropical Forest, PAS: Pastureland, PTROPF: Perennial Tropical Forest, SHSV: Shrubby Secondary Vegetation, TFOR: Temperate Forest and NW: NWrth West, NE: NWrth East, C: Centre, S: South regions.

FIGURES.

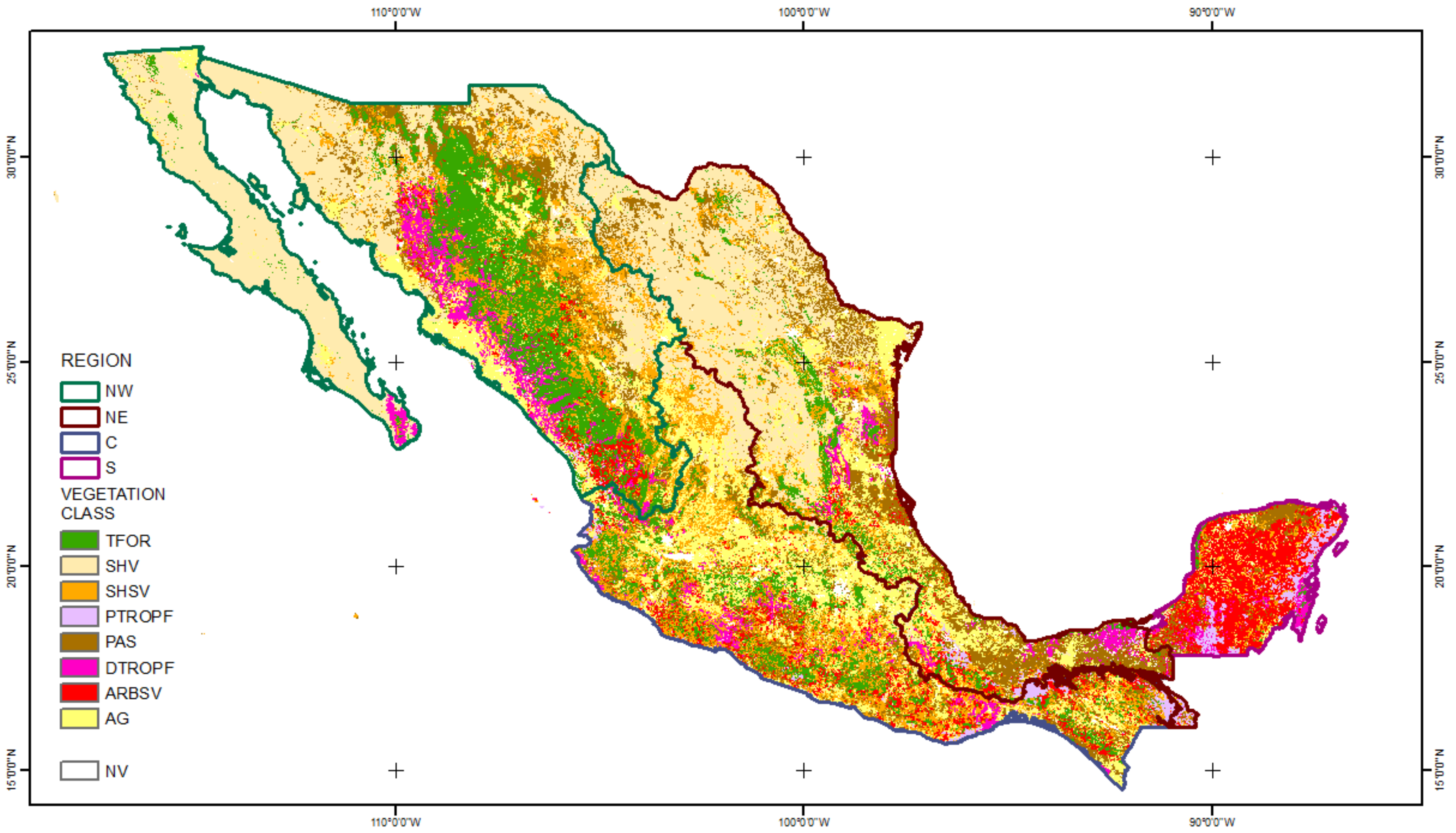

Figure 1. Map of vegetation types and regions considered in the analysis. Where: TFOR: Temperate Forest, SHV: Shrubland Vegetation, SHSV: Shrubby Secondary Vegetation, PTROPF: Perennial Tropical Forest, PAS: Pastureland, DTROPF: Deciduous Tropical Forest, ARBSV: Arboreous Secondary Vegetation, AG: Agriculture, NV: NW Vegetation; and NW: NWrth West, NE: NWrth East, C: Centre, S: South regions. Source: INEGI land use map (series V).

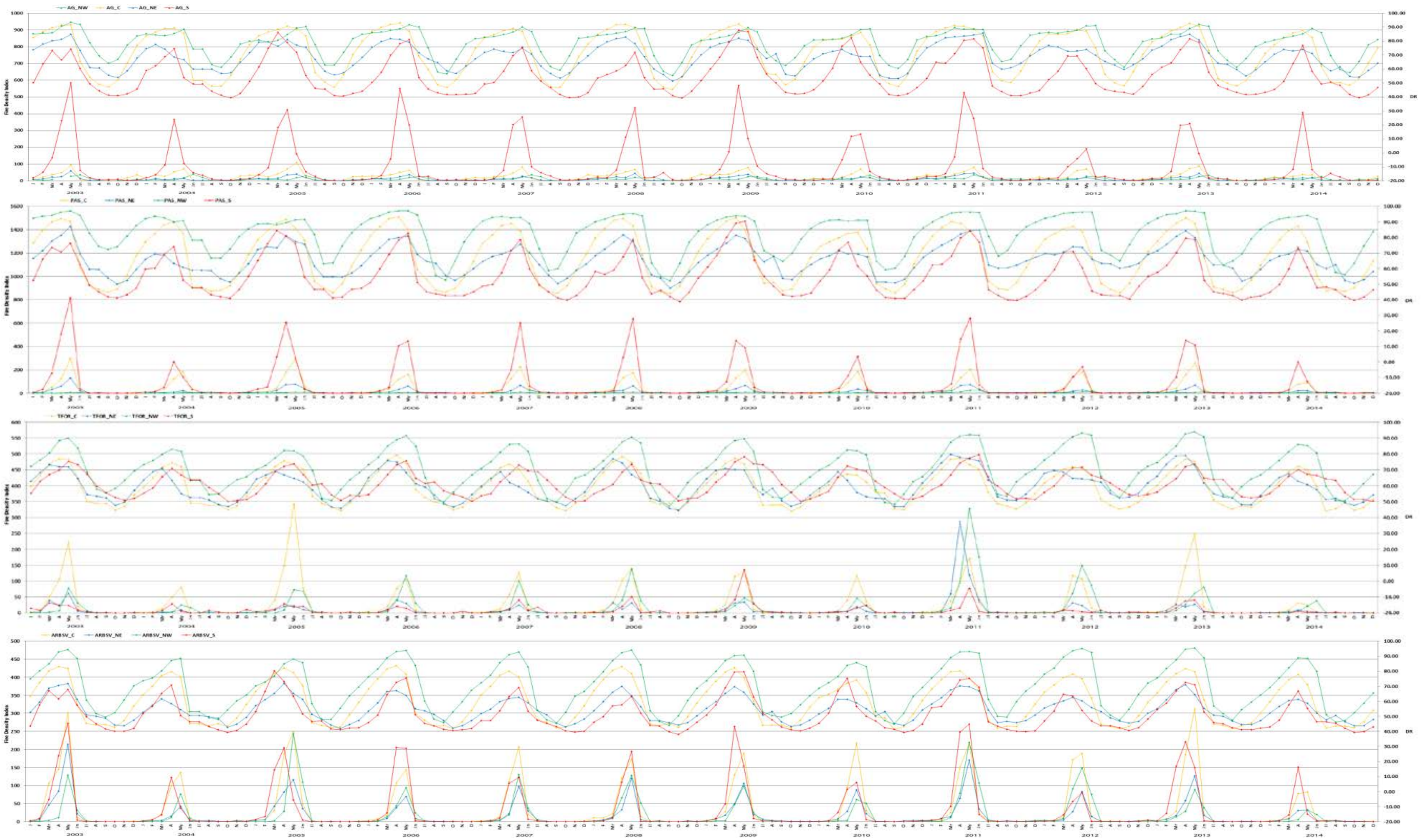

Figure 2. Observed monthly Dead Ratio (DR) (upper lines, right axis) and Fire Density Index values (lower lines, left axis) by vegetation type and region in the period 2003-2014. Where: AG: Agriculture, PAS: Pastureland, TFOR: Temperate Forest, ARBSV: Arboreous Secondary Vegetation and NW: NWrth West, NE: NWrth East, C: Centre, S: South regions. High resolution figures are included as annexes

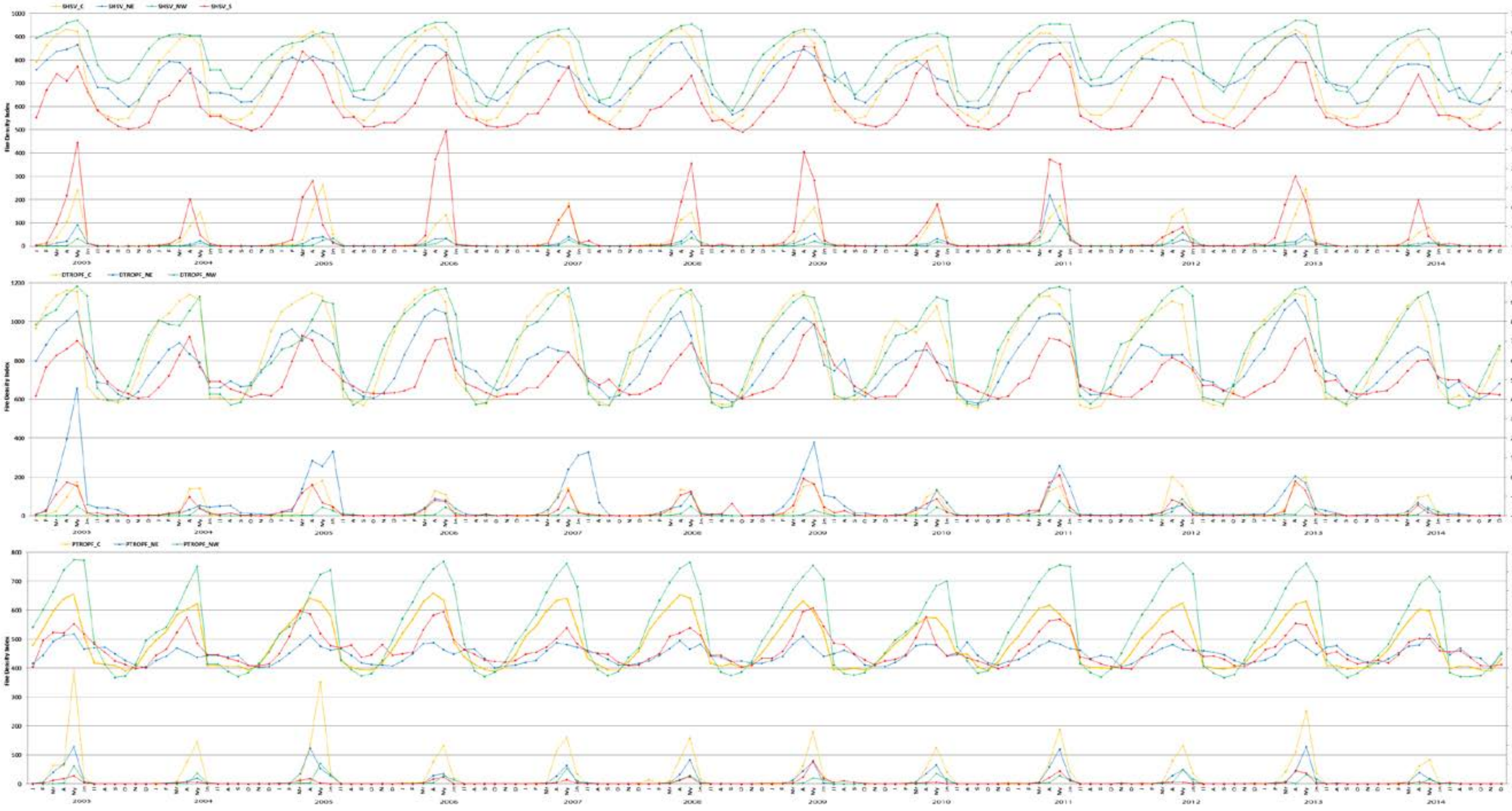

Figure 2 (continued). Observed monthly Dead Ratio (DR) (upper lines, right axis) and Fire Density Index values (lower lines, left axis) by vegetation type and region in the period 2003-2014. Where: SHSV: Shrubby Secondary Vegetation, PTROPF: Perennial Tropical Forest, DTROPF: Deciduous Tropical Forest, and NW: NWrth West, NE: NWrth East, C: Centre, S: South regions. High resolution figures are included as annexes

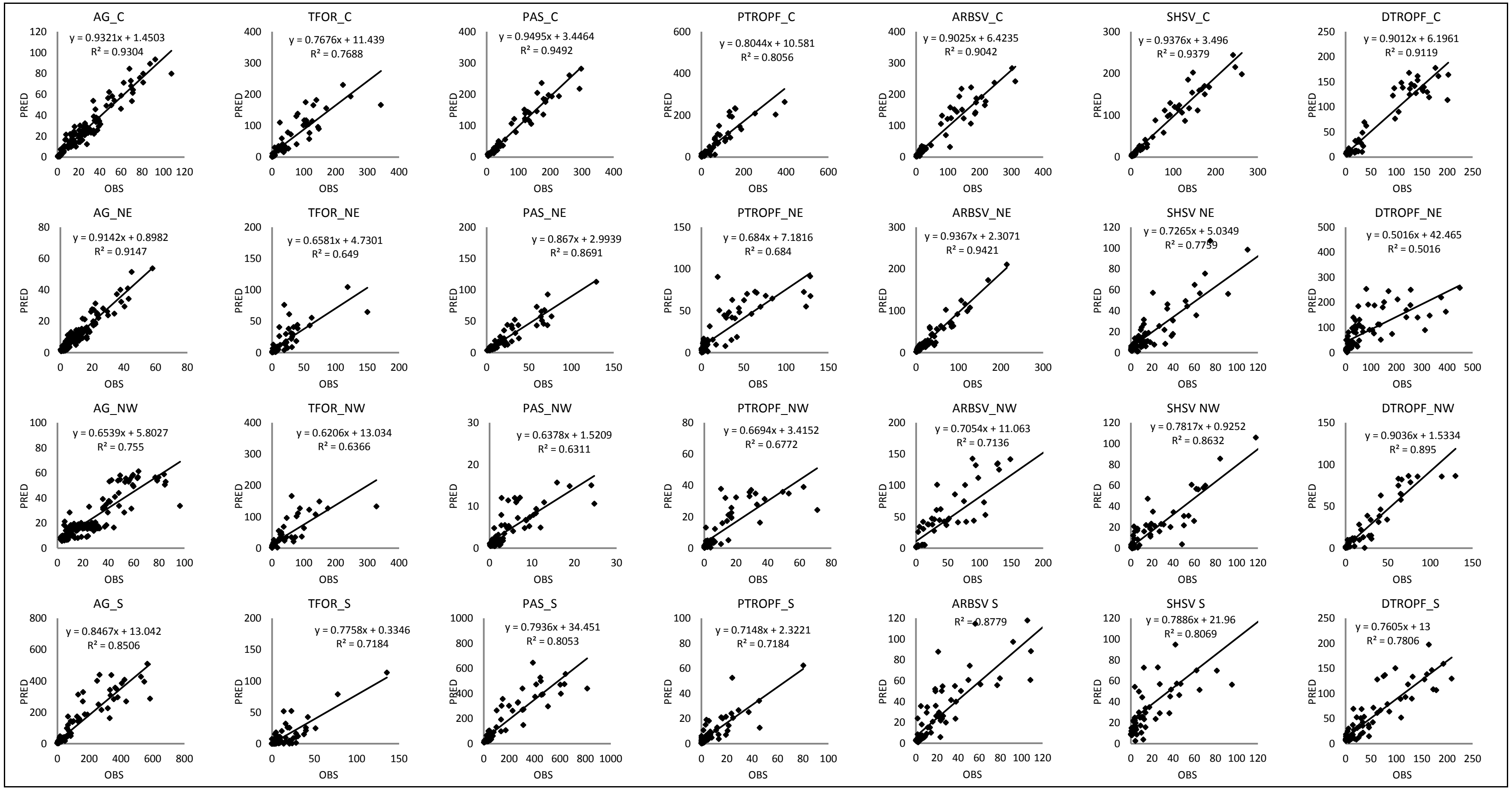

Figure 3. Predicted and observed Fire Density Index (FDI) values for each vegetation type and region. Where: PRED: predicted FDI; OBS: observed FDI; AG: Agriculture, TFOR: Temperate Forest, PAS: Pastureland, PTROPF: Perennial Tropical Forest, ARBSV: Arboreous Secondary Vegetation, SHSV: Shrubby Secondary Vegetation, DTROPF: Deciduous Tropical Forest; and NW: NWrth West, NE: NWrth

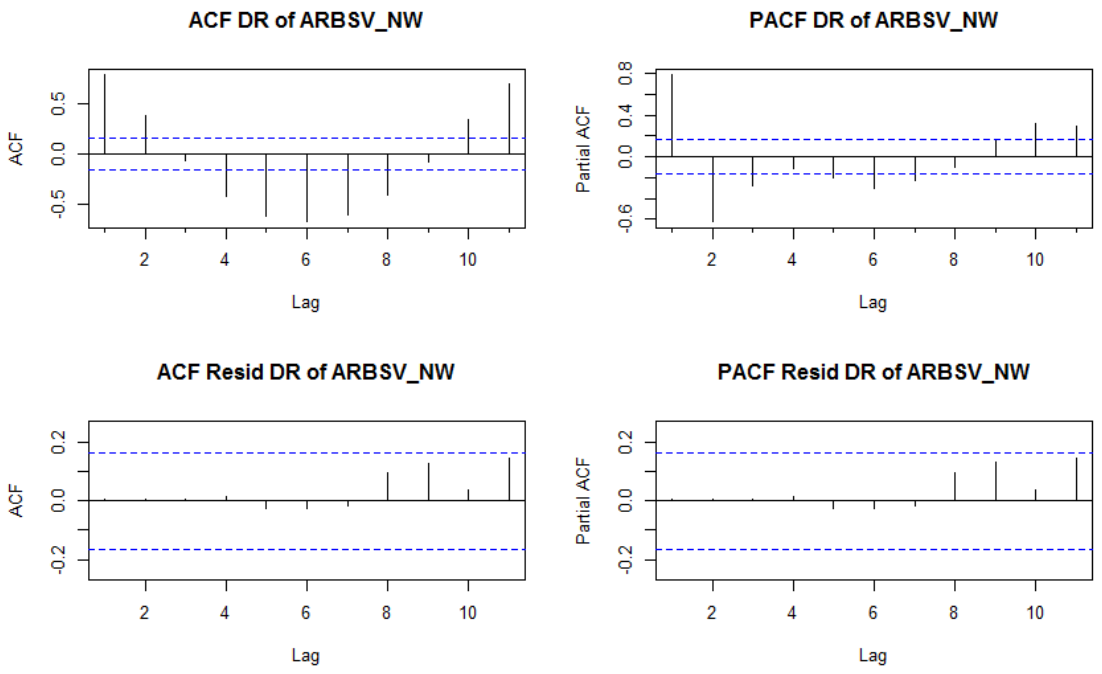

Figure 4a. Example of plots of regular and partial autocorrelation functions (ACF and PACF) of the DR data of ARBSV_NW (upper figures) and of the residuals of the modeled DR with the best fit ARIMA model (lower figures). Lines in blue mark the limits for significant autocorrelation. Plots for all vegetation types are included as annexes.

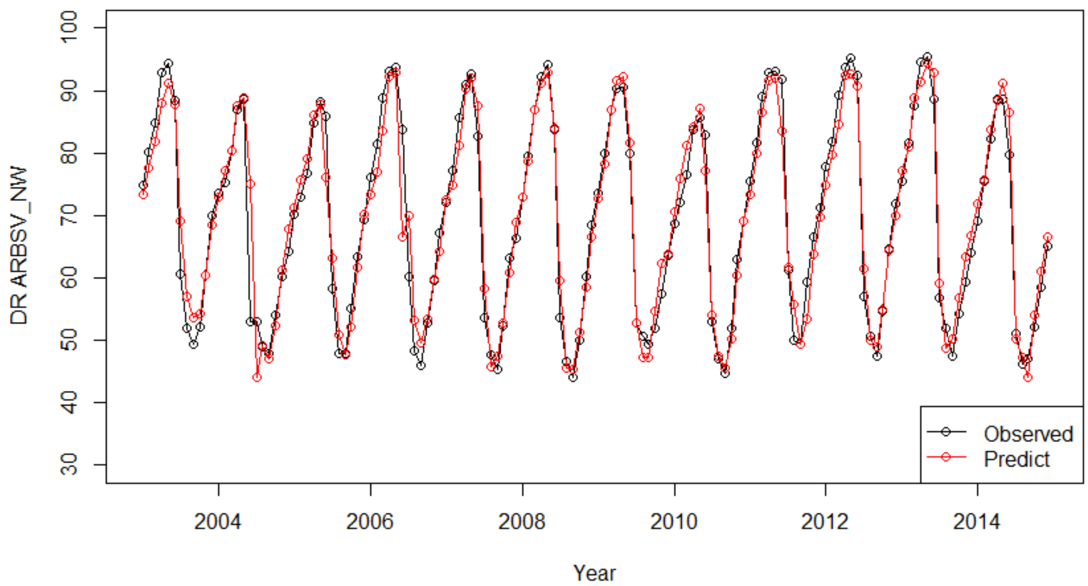

Figure 4b. Example of plots of observed and predicted DR for ARBSV_NW utilizing the best fit seasonal ARMA model. Observed data are shown in black, predicted data in red. . Plots for all vegetation types are included as annexes.

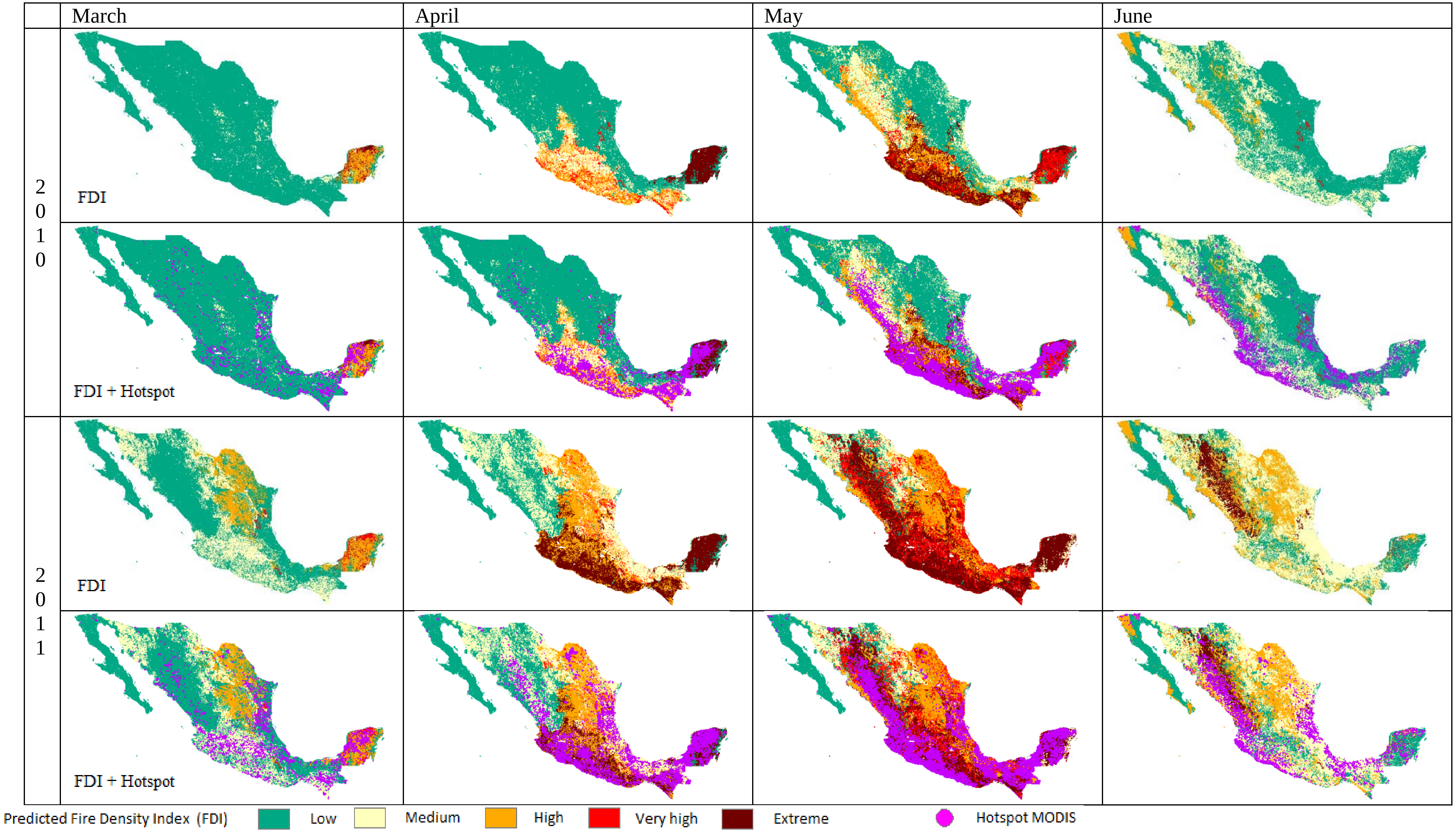

Figure 5. Maps of Predicted Fire Density Index (FDI) for the months of March, April, May and June of 2010 (upper figures) and 2011 (lower figures). Within each year, upper figures show predicted FDI maps and lower figures (*FDI + hotspots*) show maps of predicted FDI (from red to dark red) together with observed MODIS hotspots (in purple) for the corresponding month and year. FDI was scaled as follows: *Low*: FDI <25, *Medium*: 25-50; *High:* 50-75, *Very high:* 75-100, *Extreme:* FDI> 100. High resolution figures are included as annexes.